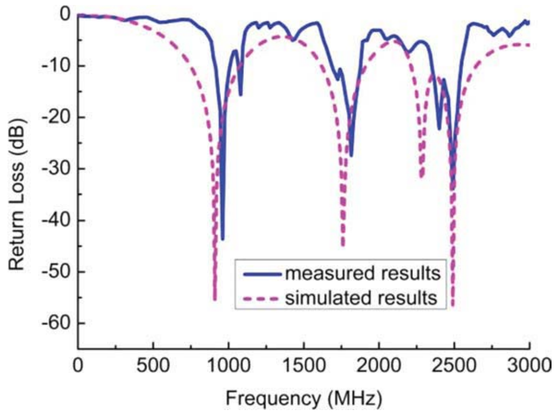

Figure 8 The measured and simulated values of return loss S_{11}. [Color figure can be viewed in the online issue, which is available at wileyonlinelibrary.com]

and 15 dB higher than that of the simulation, respectively, whereas the bandwidth about half of the simulated one. For the practical sample of this novel antenna, all measured return loss values are below -25 dB. The deviation of the measured and simulated results may lie in the fact that antenna fabrication is not as precise as possible, and also the error generated by the instruments and human beings are unavoidable.

4. CONCLUSIONS

For RFID UHF band and mobile communication application, a novel tri-bands antenna loaded with Koch fractal loops was designed on FR4 dielectric board. The simulation indicates that at three working frequency points, 910, 2490, and 1760 MHz, the return loss S_{11} values are about -52.61, -44.11, and -12.92 dB, with the bandwidths of 270, 350, and 250 MHz, respectively. Introducing a mirror array and meander-line structure, the antenna would be improved greatly. For instance, at 2490 MHz, the return loss could be decreased from -12.92 dB to about -56 dB, and the bandwidth increased from 250 to 420 MHz, with the overall size cut almost 35%. Moreover, the omnidirectional radiation pattern with 4.77 dB gain was promised. For a practical sample of this novel antenna, the measurement show that all return loss values are below -25 dB with the bandwidth bigger than 100 MHz, including all the key frequency bands.

ACKNOWLEDGMENTS

This work is supported by Fujian Provincial Key Sci-Tech Project (2010HZ0004-1) of China. The authors thank the staff members of Microwave Library and Electronic Engineering Library for helpful supports.

REFERENCES

1. P. Foster and R. Burberry, Antenna problems in RFID systems. IEE Colloquium on RFID Technology, London, UK, 1999, pp. 1–5.
2. J. Guterman, Study of fractal type printed antennas for mobile terminals Graduation Report. Instituto Superior Tecnico, Lisbon, 2003.
3. J. Guterman, A.A. Moreira, and C. Peixeiro, Dual-band miniaturized microstrip fractal antenna for a small GSM1800 + UMTS mobile handset, In: Proceedings of IEEE MELECON 2004, 2004, pp. 499–501.
4. C. Puente, J. Romeu, R. Pous, and J. Ramis, Small but long Koch fractal monopole, Electron Lett 34 (1998), 9–10.
5. C.P. Baliarda, J. Romeu, and A. Cardama, The Koch monopole: A small fractal antenna. IEEE Trans Antennas Propag 48 (2000), 1773–1781.
6. K.J. Vinoy, J.K. Abraham, and V. K. Varadan, On the relationship between fractal dimension and the performance of multi-resonant dipole antennas using Koch curves, IEEE Trans Antennas Propag 51 (2003), 2296–2303.
7. K.J. Vinoy, K.A. Jose, and V.K. Varadan, Multiband characteristics and fractal dimension of dipole antennas with Koch curve geometry. Antennas and Propagation Society International Symposium, Vol. 4, San Antonio, TX, 2002, pp. 106–109.
8. I. won Kim, The Koch island fractal microstrip patch antenna. Antennas and Propagation Society International Symposium, Vol. 2, 2001, pp. 736–739.
9. C. Borja and J. Romeu, On the behavior of Koch Island fractal boundary microstrip patch antenna, IEEE Trans Antennas Propag 51 (2003), 1281–1291.
10. N. Jin, M. Fan, and X. Zhang, L-band circular polarization microstrip antenna based on the narrow-slot fractal method. Antennas and Propagation Society International Symposium, Vol. 4, 2003, pp. 258–261.
11. D.D. Krishna and M. Gopikrishna, CPW-fed Koch fractal slot antenna for WLAN/WiMAX applications, IEEE Antennas Wirel Propag Lett 7 (2008), 389–392.
12. S.E. El-Khamy, M.A. Aboul-Dahab, and M.I. Elkashlan, A simplified Koch multiband fractal array using windowing and quantization techniques. IEEE International Symposium on Antennas and Propagation Digest, Vol. 3, 2000, pp. 1716–1719.
13. D.E. Anagnostou, A printed log-periodic Koch-dipole array (LPKDA). IEEE Antennas Wirel Propag Lett 7 (2008), 456–460.
14. S.B.D. Braatenl and P. Robert, Design of passive UHF RFID tag antennas using metamaterial-based structures and techniques. Radio frequency identification fundamentals and applications, 2010, pp. 55–68.
15. Q. Xianming and Y. Ning, A folded dipole antenna for RFID. Antennas and Propagation Society International Symposium, Vol. 1, 2004, pp.97–100,.
16. T. Wei, The design and implementation of RFID antenna. M.S. dissertation, Department of Electrical Engineering, Xiamen University, China, 2008.
17. J. Zhou, Y. Luo, and B. You, Three to two curve fractal folded dipole antenna for RFID application, Microw Opt Technol Lett 52 (2010), 1827–1830.
18. P. Hazdra, M. Capek, and J. Kracek, Optimization Tool for Fractal Patches Based on the IFS Algorithm. 3rd European Conference on Antennas and Propagation, Charleston, SC, 2009, pp. 1837–1839.
19. P. Simedra, Design and implementation of compact microstrip fractal antennas. Project Report, The University Of Western Ontario, London, Ontario, 2004.

LOW-PROFILE, SMALL-SIZE, WIRELESS WIDE AREA NETWORK HANDSET ANTENNA CLOSE INTEGRATION WITH SURROUNDING GROUND PLANE

Shu-Chuan Chen and Kin-Lu Wong
Department of Electrical Engineering, National Sun Yat-Sen University, Kaohsiung 804, Taiwan; Corresponding author: wongkl@ema.ee.nsysu.edu.tw

Received 2 June 2011

ABSTRACT: *An internal wireless wide area network (WWAN) handset antenna having a low profile of 3 mm, small footprint of 30 × 10 mm^2, and closely integrated with surrounding ground plane is presented. The antenna volume is 0.9 cm^3 only and can provide two wide-operating* *bands to cover the desired 824–960 and 1710–2170 MHz bands. The major portion of the antenna is printed on the main circuit board of the handset, and the antenna has a simple structure formed by a strip monopole and a parasitic shorted strip monopole. Two techniques are applied in the proposed design to achieve penta-band WWAN operation with a small antenna size. The first technique is to load a proper chip inductor at a proper position in the shorted strip monopole, which supports a resonant mode for the antenna's lower band with a resonant length much smaller than 0.25-wavelength. The second one is to use a band-stop matching circuit disposed on the main circuit board of the handset. The combined effects of the two techniques are discussed in this article. Also, the proposed antenna shows low near-field radiation characteristic and meets the specific absorption rate and hearing-aid compatibility requirements for practical handset applications.* Microwave Opt Technol Lett 54:623–629, 2012; View this article online at wileyonlinelibrary.com. DOI 10.1002/mop.26633

Key words: *mobile antennas; handset antennas; WWAN antennas; band-stop matching circuit*

1. INTRODUCTION

Many internal handset antennas to cover the penta-band wireless wide area network (WWAN) operation in the 824–960 and 1710–2170 MHz bands have been reported [1–13]. However, most of the reported designs did not consider close integration of the internal WWAN antenna with nearby system ground plane on the main circuit board of the handset. This is largely because the required antenna volume for the WWAN operation is still large, and hence the antenna needs to occupy the entire top or bottom edge of the system ground plane. Another reason is that the antenna structure requires some clearance or isolation distance (generally 5 mm or larger) to the nearby system ground plane such that acceptable antenna performances such as the wideband operation and good radiation efficiency over the desired operating bands can be obtained. This kind of traditional internal WWAN antennas causes a limit in its close integration with associated electronic elements in the mobile handset.

Recently, some promising internal WWAN antennas considering close integration with nearby system ground plane have been reported [14–19] in which the antennas can be disposed very close to a protruded ground extended from the system ground plane of the handset. As the protruded ground can be used to accommodate associated electronic elements in the handset, the antenna can hence be compactly embedded inside the handset and closely integrated with associated elements. However, in these reported internal WWAN antennas [14–19], they are required to be disposed at a corner of the system ground plane. That is, the protruded ground is allowed to be in close proximity to one side edge of the antenna only. In this article, we present a promising internal WWAN handset antenna with low profile (3 mm only) and small size (footprint 30×10 mm^2 only) to closely integrate with two protruded grounds (size 10×15 mm^2 each) extended from the system ground plane to surround the antenna at its two side edges.

The proposed antenna has a simple structure of a driven strip monopole and a parasitic shorted strip monopole to result in a small required antenna size. To achieve close integration of the internal WWAN antenna with surrounding ground plane in this study, two techniques are applied. The first technique is to load a proper chip inductor at a proper position in the parasitic shorted strip monopole, which supports a resonant mode for the antenna's lower band with a resonant length much smaller than 0.25-wavelength. The second one is to use a band-stop matching circuit [20] disposed on the main circuit board of the handset, which significantly enhances the antenna's lower-band bandwidth to cover the GSM850/900 operation. Also, the parasitic shorted strip monopole contributes a higher-order resonant mode to combine with the 0.25-wavelength resonant mode contributed by the driven strip monopole to achieve a wide upper band to cover the GSM1800/1900/UMTS operation. The combined effects of the two techniques lead to decrease antenna size required for the WWAN operation in the 824–960 and 1710–2170 MHz bands. The proposed antenna structure also makes it possible for the internal WWAN antenna to be closely integrated with surrounding ground plane at its two side edges. Also, the proposed antenna shows low near-field radiation characteristic and meets the specific absorption rate (SAR; Refs. 21–23) and hearing-aid compatibility (HAC; Refs. 24–26) requirements for practical handset applications. Details of the proposed antenna and the obtained results are presented and discussed.

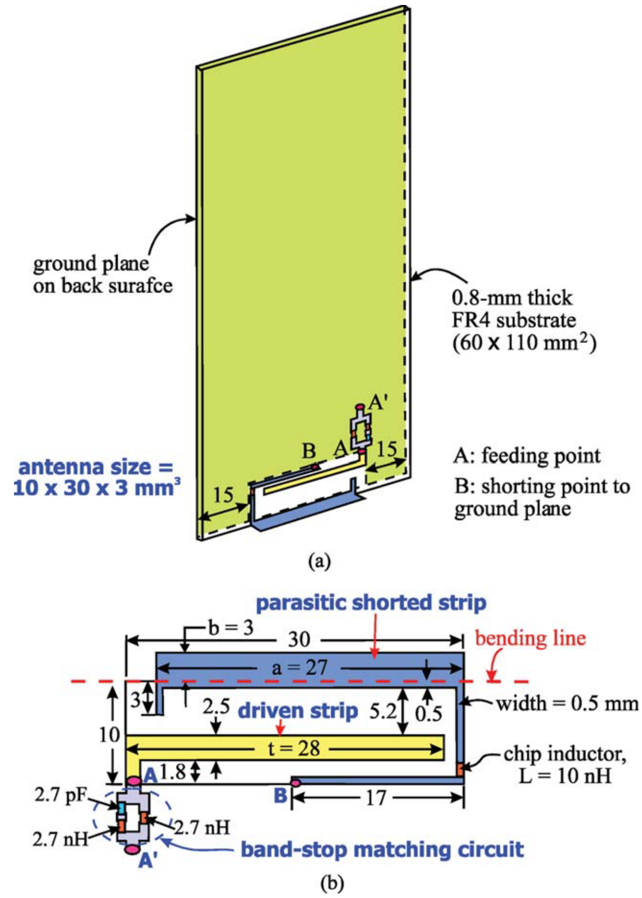

Figure 1 Geometry of the proposed WWAN handset antenna close integration with surrounding ground plane. [Color figure can be viewed in the online issue, which is available at wileyonlinelibrary.com]

2. PROPOSED ANTENNA

Figure 1(a) shows the geometry of the proposed WWAN handset antenna close integration with surrounding ground plane. Detailed dimensions of the antenna's metal pattern and the band-stop matching circuit disposed on the main circuit board are shown in Figure 1(b). The major portion of the antenna is directly printed on the front side of the main circuit board, which is a 0.8-mm thick FR4 substrate of size 110×60 mm^2, relative permittivity 4.4, and loss tangent 0.024. The footprint of the antenna is 10×30 mm^2 only and is at the center of the bottom edge of the main circuit board. The footprint is surrounded by the ground plane printed on the back side of the main circuit

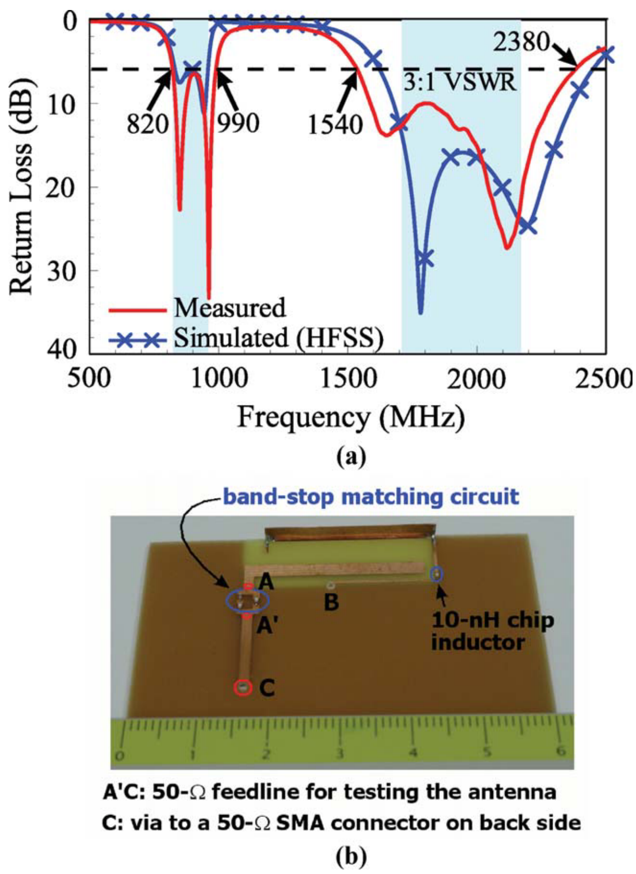

Figure 2 (a) Measured and simulated return loss of the antenna. (b) Photo of the fabricated antenna. [Color figure can be viewed in the online issue, which is available at wileyonlinelibrary.com]

board. At the two side edges of the footprint, there are two protruded grounds of size 10×15 mm^2 extended from the main ground plane. As mentioned earlier, the two protruded grounds can be used to accommodate associated electronic elements in the handset, leading to compact integration of the internal WWAN antenna inside the handset.

The antenna's metal pattern mainly comprises a driven strip monopole and a parasitic shorted strip monopole. The driven strip monopole has a length of about 31 mm and can contribute a resonant mode in the antenna's desired upper band. The parasitic shorted strip monopole has a length of about 60 mm and is short-circuited to the ground plane on the back side of the main circuit board through a via-hole at point B (shorting point). By loading a 10-nH chip inductor away from the shorting point B with a distance of 17 mm, at which a current null occurs for the excited higher-order resonant mode of the shorted strip monopole, the 0.25-wavelength resonant mode of the shorted strip monopole can be shifted to lower frequencies at about 850 MHz with the higher-order resonant mode of the shorted strip monopole exited in the antenna's desired upper band very slightly affected. The higher-order resonant mode of the shorted strip monopole combines with the resonant mode contributed by the driven strip monopole to form a wide upper band for the antenna to cover the GSM1800/1900/UMTS operation (1710–2170 MHz). The chip-inductor loading method applied in this study makes it convenient to adjust the frequency ratio of the first two resonant modes of the shorted strip monopole.

Near the open end of the shorted strip monopole, the strip width is widened by connecting a metal strip of length (*a*) 27 mm and width (*b*) 3 mm that is cut from a 0.2-mm-thick copper plate and then connected to the antenna's printed metal pattern on the main circuit board. This widened section mainly helps achieve enhanced bandwidth in the antenna's lower band. Further, using a band-stop matching circuit [20] disposed on the main circuit board, which is formed by a 2.7-nH chip inductor in parallel connection with a 2.7-pF chip capacitor and a 2.7-nH chip inductor, a parallel resonance can be generated at about 1000 MHz. The generated parallel resonance is at the high-frequency tail of the 0.25-wavlength resonant mode of the shorted strip monopole and can effectively improve the impedance matching of the same to generate an additional resonance (zero reactance) nearby, thereby resulting in a dual-resonance resonant mode to achieve a much wider bandwidth to cover the GSM850/900 operation (824–960 MHz).

3. RESULTS OF PROPOSED ANTENNA

Figure 2(a) shows the measured and simulated return loss of the proposed antenna fabricated as shown in Figure 2(b). The simulated results are obtained using full-wave electromagnetic field simulator high-frequency structure simulator [27], and agreement between the simulation and measurement is seen. The measured impedance bandwidth based on 3:1 VSWR, which is widely used as the design specification of the internal WWAN handset antennas, is seen to cover the desired 824–960 and 1710–2170 MHz bands for the penta-band WWAN operation.

To analyze the operating principle of the antenna, Figure 3 shows a comparison of the simulated return loss for the

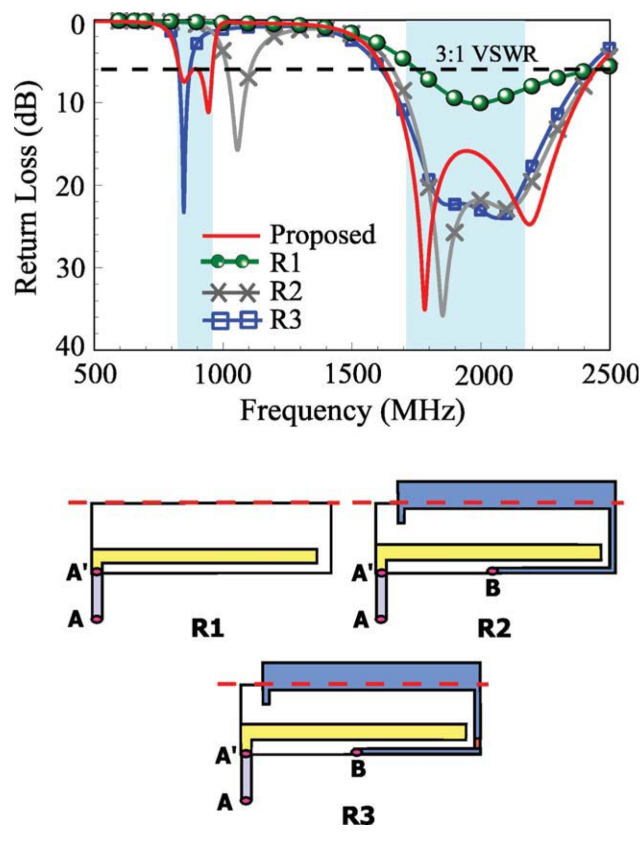

Figure 3 Comparison of the simulated return loss for the proposed antenna, the case with the driven strip monopole only (R1), the case with the driven strip monopole and simple shorted strip monopole (R2), and the case with the driven strip monopole and chip-inductor-loaded shorted strip monopole (R3). [Color figure can be viewed in the online issue, which is available at wileyonlinelibrary.com]

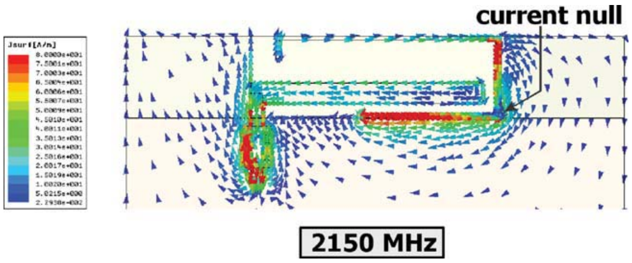

Figure 4 Simulated surface current distributions at 2150 MHz for the proposed antenna. [Color figure can be viewed in the online issue, which is available at wileyonlinelibrary.com]

proposed antenna, the case with the driven strip monopole only (R1), the case with the driven strip monopole and simple shorted strip monopole (R2), and the case with the driven strip monopole and chip-inductor-loaded shorted strip monopole (R3). For R1, there is one resonant mode occurred at about 2000 MHz, whereas for R2, two additional resonant modes at about 1100 and 2150 MHz are generated owing to the shorted strip monopole. The resonant mode at about 2150 MHz combines with the one contributed by the driven strip monopole form the antenna's upper band. By loading a 10-nH chip inductor to the shorted strip monopole, the resonant mode at about 1100 MHz can be shifted to lower frequencies at about 850 MHz. However, the obtained bandwidth is narrow and far from covering the GSM850/900 operation. Also, note that the chip-inductor loading generally shows very small effects on the antenna's upper band. This is mainly because the chip inductor in this study is loaded in the vicinity where there is current null for the excited surface currents of the higher-order resonant mode of the shorted strip monopole (see the simulated surface current distributions in Figure 4, at 2150 MHz for the antenna). Hence, very small effects on the higher-order resonant mode of the shorted strip monopole can be obtained. Then, by further adding the band-stop matching circuit to R3 to form the proposed antenna, a dual-resonance excitation of the 0.25-wavelength mode of the shorted strip monopole is obtained, which shows a wide-operating band to cover the GSM850/900 operation.

To show it more clearly for the effects of the band-stop matching circuit, Figure 5 presents the simulated return loss for the proposed antenna and the case without the band-stop matching circuit (R3 in Fig. 3). It is clear to see that a parallel resonance at about 1000 MHz is generated, which leads to an additional resonance occurred at about 940 MHz. This additional resonance results in the dual-resonance excitation seen in Figure 3 for the antenna's lower band. Also, small effects on the

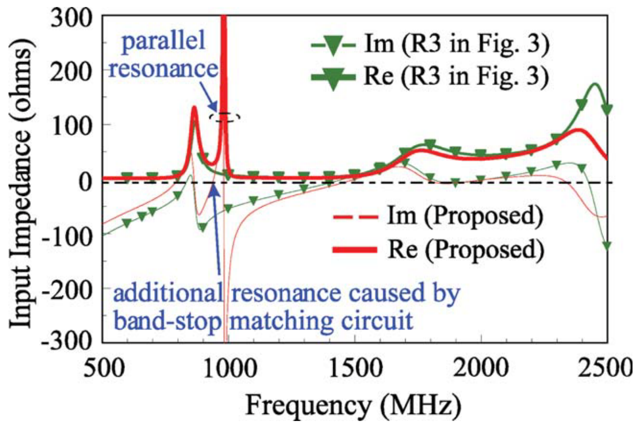

Figure 5 Simulated return loss for the proposed antenna and the case without the band-stop matching circuit (R3 in Fig. 3). [Color figure can be viewed in the online issue, which is available at wileyonlinelibrary.com]

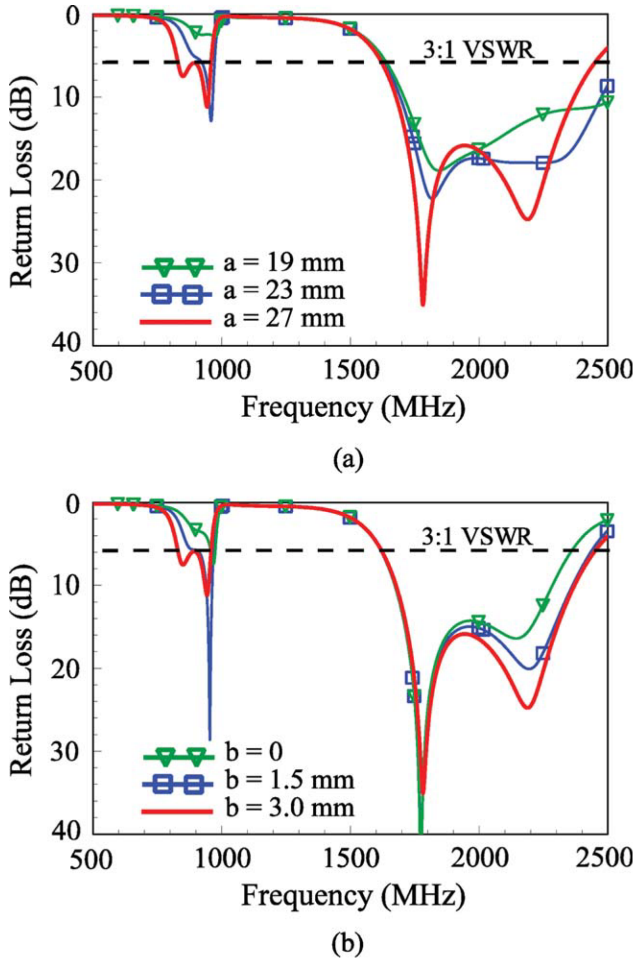

Figure 6 Simulated return loss as a function of (a) the length *a* and (b) the width *b* of the widened section in the shorted strip monopole for the proposed antenna. [Color figure can be viewed in the online issue, which is available at wileyonlinelibrary.com]

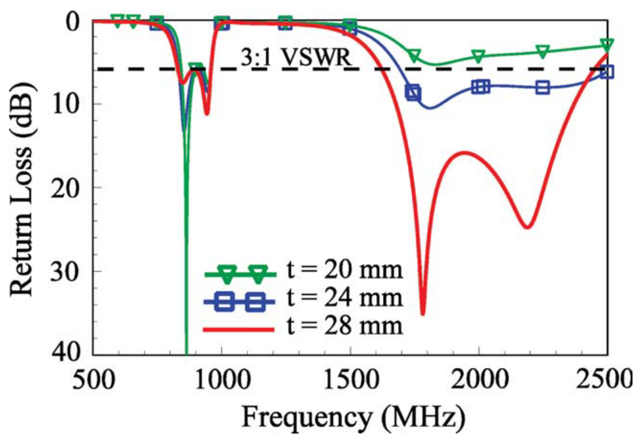

Figure 7 Simulated return loss as a function of the length *t* in the driven strip monopole for the proposed antenna. [Color figure can be viewed in the online issue, which is available at wileyonlinelibrary.com]

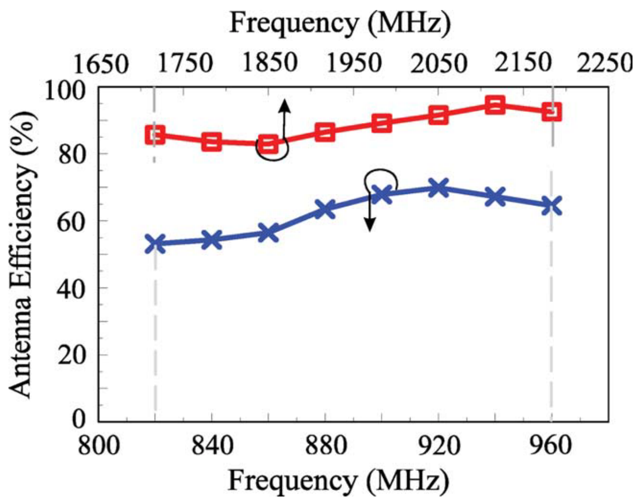

Figure 8 Measured antenna efficiency (mismatching loss included) of the proposed antenna. [Color figure can be viewed in the online issue, which is available at wileyonlinelibrary.com]

impedance matching of the frequencies in the desired upper band are seen.

Figure 6 shows the simulated return loss as a function of the length a and the width b of the widened section in the shorted strip monopole for the proposed antenna. Results of the simulated return loss for the length a varied from 19 to 27 mm are presented in Figure 6(a), and those for the width b varied from 0 to 3 mm are presented in Figure 6(b). It is seen that the resonant mode at about 850 MHz (0.25-wavelength mode of the shorted strip monopole) is greatly affected, causing large bandwidth decrease in the antenna's lower band. Large effects on the resonant mode at about 2150 MHz (higher-order mode of the shorted strip monopole) are also seen. However, the obtained impedance bandwidth of the antenna's upper band can still cover the desired operating band of 1710–2170 MHz.

Figure 7 shows the simulated return loss as a function of the length t in the driven strip monopole for the proposed antenna. Results for the length t varied from 20 to 28 mm are presented. In this case, relatively small effects on the antenna's lower band are seen. This behavior is reasonable, as the lower band is

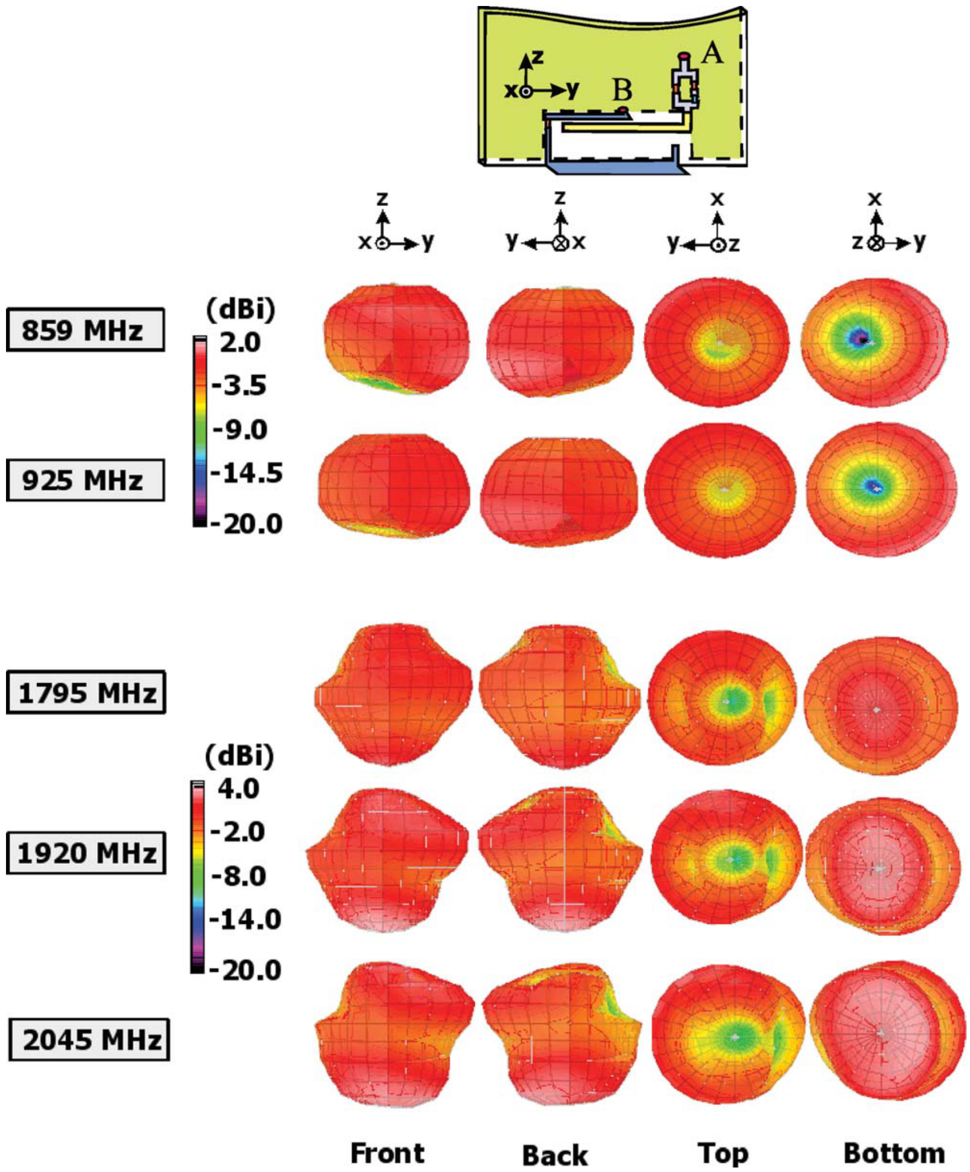

Figure 9 Measured three-dimensional total-power radiation patterns of the proposed antenna. [Color figure can be viewed in the online issue, which is available at wileyonlinelibrary.com]

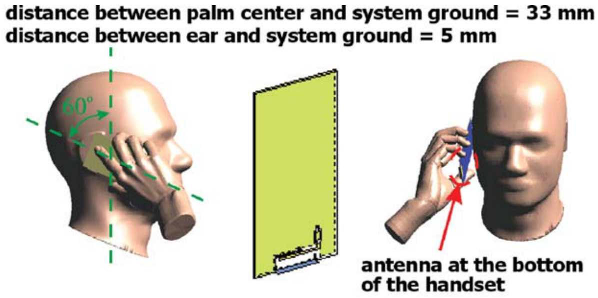

Frequency (MHz)		859	925	1795	1920	2045
1-g SAR (W/kg)	head only	0.61	0.67	0.29	0.26	0.29
	hand only	1.30	1.08	1.10	1.09	0.94
	head and hand	1.30	1.08	1.10	1.09	0.94
Return loss (dB)	head only	10.3	7.2	23.3	14.5	11.6
	hand only	12.1	7.3	13.1	27.2	20.8
	head and hand	10.8	6.9	11.3	20.4	23.4

Figure 10 SAR simulation model and the simulated SAR values for 1-g tissue. [Color figure can be viewed in the online issue, which is available at wileyonlinelibrary.com]

mainly related to the shorted strip monopole and the band-stop matching circuit. For the antenna's upper band, very large effects are observed. This behavior is in part, because the first resonant mode in the upper band is contributed by the driven strip monopole. Also, probably, because the variations in the length t will cause some distance variations between the open end of the driven strip monopole and the null current location (where the chip inductor is loaded) of the excited surface current distribution of the higher-order mode of the shorted strip monopole, the impedance matching of the second mode in the antenna's upper band is greatly affected. Hence, large effects on both the two resonant modes in the upper band are seen for the variations in the length t.

The measured antenna efficiency of the proposed antenna is shown in Figure 8. The antenna efficiency includes the mismatching loss and was measured in a far-field anechoic chamber. Over the lower and upper bands, the antenna efficiency is about 56–76% and 82–92%, respectively. As the antenna efficiency larger than about 50% is sufficient for practical applications, the measured results indicate that acceptable antenna efficiency is obtained for practical applications. The measured three-dimensional total-power radiation patterns of the antenna are also plotted in Figure 9. The radiation patterns seen in four different directions (front, back, top, and bottom directions) at each testing frequency are shown. The measured radiation patterns at lower frequencies (859 and 925 MHz) and higher frequencies (1795, 1920, and 2045 MHz) are similar to those observed for many internal WWAN handset antennas [28–30].

Figure 10 shows the SAR simulation model and the simulated 1-g SAR values for the proposed antenna. The SAR values for 1-g tissue in the three cases of the head only, the hand only, and the head and hand are studied using the SAR simulation model provided by SEMCAD X version 14 [31]. The return loss for the three cases at each testing frequency is also given in the figure. It is seen that for the head only, the SAR values are much less than those for the other two cases in which the obtained SAR values are the same. The results indicate that the SAR values are dominated by the user's hand. However, for the proposed antenna, the SAR values for the three cases are all less than the limit of 1.6 W/kg [21].

Figure 11 shows the HAC simulation model and the simulated HAC results. The HAC simulation model provided by SEMCAD X version 14 [31] is also used. The testing power at each testing frequency is given in the figure. The obtained HAC results are rated to be at least M3 for both the E-field and the H-field, indicating that the proposed antenna meets the HAC requirement for practical applications [24]. The differences between the obtained E-field (H-field) strength and the limit of the E-field (H-field) HAC M3 category are given by ΔE and ΔH in the figure. The good results on the HAC testing are related to the presence of the two protruded grounds at two side edges of the antenna, which can attract some strong excited surface currents that are originally on the main ground plane when the protruded grounds are not present [17]. The simulated surface currents at typical frequencies on the system ground plane shown in Figure 12 are very weak near the top edge of the system ground plane where the acoustic output is located and can support the observation of good HAC results obtained in this study.

4. CONCLUSIONS

An internal WWAN handset antenna occupying a volume of 0.9 cm^3 only and closely integrating with surrounding ground plane at its two side edges has been proposed. The techniques applied in the proposed antenna to achieve small antenna volume yet wideband operation to cover the 824–960 and 1710–2170 MHz bands have been studied. Good radiation characteristics for frequencies over the WWAN bands have been obtained. Near-field radiation characteristics of the antenna have also been analyzed.

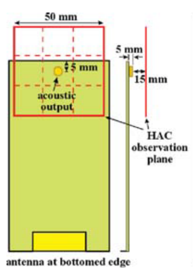

Operating band, Testing freq. (MHz)		GSM, 859	GSM, 925	GSM, 1795	GSM, 1920	UMTS, 2045
E-field (V/m)	(dB)	46.4 (M3)	46.4 (M3)	37.1 (M3)	35.7 (M3)	27.6 (M4)
	△E	-2.1	-2.1	-1.4	-2.8	-13.4
H-field (A/m)	(dB)	-9.5 (M4)	-9.0 (M4)	-13.0 (M3)	-13.4 (M3)	-22.6 (M4)
	△H	-7.6	-7.1	-1.1	-1.5	-13.2
Testing power (W)	dBm	33	33	30	30	21

Figure 11 HAC simulation model and the simulated HAC results. ΔE and ΔH indicate, respectively, the decrease in the E-field and H-field strengths owing to the presence of the two protruded grounds at two side edges of the antenna. [Color figure can be viewed in the online issue, which is available at wileyonlinelibrary.com]

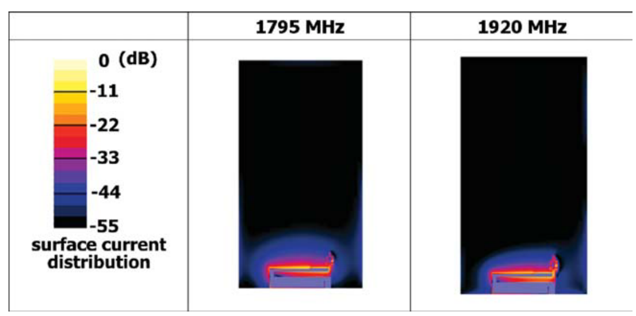

Figure 12 Simulated surface current distributions on the system ground plane. [Color figure can be viewed in the online issue, which is available at wileyonlinelibrary.com]

The obtained SAR values for 1-g tissue meet the limit of 1.6 W/kg, even for the case including the user's hand, and the obtained HAC results are rated to be in the M3 or M4 category. The obtained results indicate that the proposed antenna is promising for practical handset applications especially for slim handset applications.

REFERENCES

1. H. Rhyu, J. Byun, F.J. Harackiewicz, M.J. Park, K. Jung, D. Kim, N. Kim, T. Kim, and B. Lee, Multi-band hybrid antenna for ultra-thin mobile phone applications, Electron Lett 45 (2009), 773–774.
2. C.H. Chang and K.L. Wong, Printed λ/8-PIFA for penta-band WWAN operation in the mobile phone, IEEE Trans Antennas Propag 57 (2009), 1373–1381.
3. T.W. Kang and K.L. Wong, Chip-inductor-embedded small-size printed strip monopole for WWAN operation in the mobile phone, Microwave Opt Technol Lett 51 (2009), 966–971.
4. J.Y. Sze and Y.F. Wu, A compact planar hexa-band internal antenna for mobile phone, Prog Electromagn Res 107 (2010), 413–425.
5. C.L. Liu, Y.F. Lin, C.M. Liang, S.C. Pan, and H.M. Chen, Miniature internal penta-band monopole antenna for mobile phones, IEEE Trans Antennas Propag 58 (2010), 1008–1011.
6. K.L. Wong and S.C. Chen, Printed single-strip monopole using a chip inductor for penta-band WWAN operation in the mobile phone, IEEE Trans Antennas Propag 58 (2010), 1011–1014.
7. S.C. Chen and K.L. Wong, Bandwidth enhancement of coupled-fed on-board printed PIFA using bypass radiating strip for eight-band LTE/GSM/UMTS slim mobile phone, Microwave Opt Technol Lett 52 (2010), 2059–2065.
8. F.H. Chu and K.L. Wong, Simple planar printed strip monopole with a closely-coupled parasitic shorted strip for eight-band LTE/GSM/UMTS mobile phone, IEEE Trans Antennas Propag 58 (2010), 3426–3431.
9. K.J. Kim, S.H. Lee, B.N. Kim, J.H. Jung, and Y.J. Yoon, Multi-band antenna with coupling feed structure for mobile handset applications, In: IEEE Antennas and Propagation Society International Symposium, Toronto, Canada, 2010, pp. 1–4.
10. C.W. Chiu, C.H. Chang, and Y.J. Chi, A compact folded loop antenna for LTE/GSM band mobile phone applications, In: International Conference on Electromagnetics in Advanced Applications, Sydney, Australia, 2010, pp. 382–385.
11. K.L. Wong and Y.W. Chang, Internal eight-band WWAN/LTE handset antenna using loop shorting strip and chip-capacitor-loaded feeding strip for bandwidth enhancement, Microwave Opt Technol Lett 53 (2011), 1217–1222.
12. S.C. Chen and K.L. Wong, Planar strip monopole with a chip-capacitor-loaded loop radiating feed for LTE/WWAN slim mobile phone, Microwave Opt Technol Lett 53 (2011), 952–958.
13. C.Y.D. Sim, P.C. Cheng, and C.H. Lee, Low-profile multiband planar hybrid antenna design for mobile handset applications, Microwave Opt Technol Lett 53 (2011), 910–915.
14. K.L. Wong, T.W. Kang, and M.F. Tu, Antenna array for LTE/WWAN and LTE MIMO operations in the mobile phone, Microwave Opt Technol Lett 53 (2011), 1569–1573.
15. F.H. Chu and K.L. Wong, On-board small-size printed LTE/WWAN mobile handset antenna closely integrated with nearby system ground plane, Microwave Opt Technol Lett 53 (2011), 1336–1343.
16. K.L. Wong, W.Y. Chen, and T.W. Kang, On-board printed coupled-fed loop antenna in close proximity to the surrounding ground plane for penta-band WWAN mobile phone, IEEE Trans Antennas Propag 59 (2011), 751–757.
17. S.C. Chen and K.L. Wong, Hearing aid-compatible internal LTE/WWAN bar-type mobile phone antenna, Microwave Opt Technol Lett 53 (2011), 774–781.
18. K.L. Wong, M.F. Tu, C.Y. Wu, and W.Y. Li, On-board 7-band WWAN/LTE antenna with small size and compact integration with nearby ground plane in the mobile phone, Microwave Opt Technol Lett 52 (2010), 2847–2853.
19. K.L. Wong and C.H. Chang, On-board small-size printed monopole antenna integrated with USB connector for penta-band WWAN mobile phone, Microwave Opt Technol Lett 52 (2010), 2523–2527.
20. Y.W. Chi and K.L. Wong, Very-small-size folded loop antenna with a band-stop matching circuit for WWAN operation in the mobile phone, Microwave Opt Technol Lett 51 (2009), 808–814.
21. American National Standards Institute (ANSI), Safety levels with respect to human exposure to radio-frequency electromagnetic field, 3 kHz to 300 GHz, ANSI/IEEE standard C95.1, April 1999.
22. Y.W. Chi and K.L. Wong, Compact multiband folded loop chip antenna for small-size mobile phone, IEEE Trans Antennas Propag 56 (2008), 3797–3803.
23. Y.W. Chi and K.L. Wong, Quarter-wavelength printed loop antenna with an internal printed matching circuit for GSM/DCS/PCS/UMTS operation in the mobile phone, IEEE Trans Antennas Propag 57 (2009), 2541–2547.
24. American National Standard for method of measurement of compatibility between wireless communication devices and hearing aids (ANSI C63.19-2007, revision ANSI C63.19–2006), American National Standards Institute, New York, 2007.
25. T. Yang, W.A. Davis, W.L. Stutzman, and M.C. Huynh, Cellular-phone and hearing-aid interaction: An antenna solution, IEEE Antennas Propag Mag 50 (2008), 51–65.
26. K.L. Wong and M.F. Tu, Hearing aid-compatible internal penta-band antenna for clamshell mobile phone, Microwave Opt Technol Lett 51 (2009), 1408–1413.
27. ANSYS HFSS, Ansoft Corp., Pittsburgh, PA, Available at: http://www.ansys.com/products/hf/hfss/.
28. K.L. Wong, P.W. Lin, and C.H. Chang, Simple printed monopole slot antenna for penta-band WWAN operation in the mobile handset, Microwave Opt Technol Lett 53 (2011), 1399–1404.
29. K.L. Wong, W.Y. Chen, C.Y. Wu, and W.Y. Li, Small-size internal eight-band LTE/WWAN mobile phone antenna with internal distributed LC matching circuit, Microwave Opt Technol Lett 52 (2010), 2244–2250.
30. C.T. Lee and K.L. Wong, Planar monopole with a coupling feed and an inductive shorting strip for LTE/GSM/UMTS operation in the mobile phone, IEEE Trans Antennas Propag 58 (2010), 2479–2483.
31. SPEAG SEMCAD, Schmid & Partner Engineering AG, Germany, Available at: http://www.semcad.com.

WIDEBAND AND COMPACT ERBIUM-DOPED FIBER AMPLIFIER USING PARALLEL DOUBLE-PASS CONFIGURATION

B. A. Hamida,[1] X. S. Cheng,[2] S. W. Harun,[2,3] A. W. Naji,[1] H. Arof,[2] S. Khan,[1] W. Alkhateeb,[1] and H. Ahmad[3]

[1] Optoelectronics Laboratory, Department of Electrical and Computer Engineering, Faculty of Engineering, International Islamic University Malaysia (IIUM), 53100 Gombak, Kuala Lumpur, Malaysia

[2] Department of Electrical Engineering, Faculty of Engineering, University of Malaya, 50603 Kuala Lumpur, Malaysia; Corresponding author: swharun@um.edu.my

[3] Photonics Research Center, University of Malaya, 50603 Kuala Lumpur, Malaysia

Received 15 May 2011

ABSTRACT: *In this article, a wide-band erbium doped fiber amplifier (EDFA) that operates in both C- and L-band wavelength regions is demonstrated. The amplifier employs two pieces of 1.5 m and 9 m-long erbium doped fibers (EDFs) optimized for C-band and L-band operations, respectively, in double-pass parallel configuration to achieve a wideband operation from 1530 to 1605 nm. The chirp fiber Bragg grating is used in both stages to allow a double propagation of signal*